



## Dielectric properties of bismuth titanate ceramics containing $\text{SiO}_2$ and $\text{Nd}_2\text{O}_3$ as additives<sup>#</sup>

Stanislav S. Slavov<sup>1,\*</sup>, Milena Z. Krapchanska<sup>2</sup>, Elena P. Kashchieva<sup>1</sup>, Svetlin B. Parvanov<sup>1</sup>, Yanko B. Dimitriev<sup>3</sup>

<sup>1</sup>Department of Physics, University of Chemical Technology and Metallurgy, 8 Kl. Ohridski Blvd., 1756 Sofia, Bulgaria

<sup>2</sup>Bulgarian Academy of Sciences, Institute of Electrochemistry and Energy Systems, Acad. G. Bonchev Str., Bl. 10, 1113 Sofia, Bulgaria

<sup>3</sup>Department of Silicate Technology, University of Chemical Technology and Metallurgy, 8 Kl. Ohridski Blvd., 1756 Sofia, Bulgaria

Received 27 December 2011; received in revised form 19 June 2012; accepted 4 July 2012

### Abstract

Bismuth-titanate ceramics containing  $\text{SiO}_2$  and  $\text{Nd}_2\text{O}_3$  as additives are synthesized by melt quenching method in the system  $\text{Bi}_2\text{O}_3\text{-TiO}_2\text{-Nd}_2\text{O}_3\text{-SiO}_2$  in the temperature range of 1250–1500 °C. The phase composition of the obtained materials is determined by X-ray diffraction analysis and energy dispersive spectroscopy. Using scanning electron microscopy different microstructures are observed in the samples depending on the composition. Different values of conductivity, dielectric losses and relative permittivity are obtained depending on the composition. It is established that all investigated samples are dielectric materials with conductivity between  $10^9$  and  $10^{-13} (\Omega\cdot\text{cm})^{-1}$  at room temperature, dielectric permittivity from 1000 to 3000 and dielectric losses  $\text{tg}\delta$  between 0.0002 and 0.1.

**Keywords:** bismuth titanate, melt quenching, microstructure, electrical properties

### 1. Introduction

Aurivillius family oxides including  $\text{Bi}_4\text{Ti}_3\text{O}_{12}$  are of great interest in the last years due to their potential for electronic applications as transducers, capacitors, and acoustic piezo-sensors with high temperature piezoelectric properties (because of its high Curie temperature) [1,2]. Many techniques have been employed for preparing a layered structure of bismuth titanate phases including powders and bulk ceramics: molten salt synthesis, co-precipitation, reactive calcinations, sol-gel synthesis, mechanochemical method and others. Between them the crystallisation from melts or glasses [3–6] gives the possibility for easy control of the particle size distribution, morphology and crystallographic orientation. It is well known, that the phase formation and

the properties of  $\text{Bi}_4\text{Ti}_3\text{O}_{12}$  ceramics are strongly influenced not only by the method of preparation, but also by the type and portion of additives. The introduction of  $\text{Nd}_2\text{O}_3$  as an additive allows the synthesis of materials with improved dielectric and ferroelectric properties, such as high dielectric constant, low dielectric losses, high remnant polarisation and high resistance to fatigue [7–18]. The other advantage of  $\text{Nd}_2\text{O}_3$  addition is the existence of solid solutions in the system  $\text{Bi}_2\text{O}_3\text{-TiO}_2\text{-Nd}_2\text{O}_3$ . Thus, Kunej *et al.* [19] described the solubility limits of three solid-solutions:  $\text{Bi}_{(1.6-1.08x)}\text{Nd}_x\text{Ti}_2\text{O}_{(6.4+0.3x)}$ , ( $0.25 < x < 0.96$ ),  $\text{Nd}_{2-x}\text{Bi}_x\text{Ti}_2\text{O}_7$ , ( $0 < x < 0.35$ ), and  $\text{Bi}_{4-x}\text{Nd}_x\text{Ti}_3\text{O}_{12}$ , ( $0 < x < 2.6$ ).

In the previous works [20,21] it has been shown that the introduction of 20–40 mol%  $\text{SiO}_2$  simulates the partial amorphisation of the samples. The main established phases in the super cooled melt are either  $\text{Bi}_2\text{Ti}_2\text{O}_7$  and  $\text{Bi}_4\text{Ti}_3\text{O}_{12}$  or only  $\text{Bi}_4\text{Ti}_3\text{O}_{12}$ , depending on the cooling rate and composition. The other important result was that the simultaneous introduction of  $\text{SiO}_2$  and  $\text{Nd}_2\text{O}_3$  as

<sup>#</sup> Paper presented at Conference for Young Scientists - 9<sup>th</sup> Students' Meeting, SM-2011, Novi Sad, Serbia, 2011

\* Corresponding author: tel: +35 92 8163 450

fax: +35 92 8685 488, e-mail: stanislavslavov@hotmail.com

additives [21] in the bismuth-titanate ceramics changes the glass-formation ability and electrical properties. These results motivated us to continue our experiments in this field. The purposes of the present work are to prepare polycrystalline or glass-ceramic materials in the system  $\text{Bi}_2\text{O}_3\text{-TiO}_2\text{-SiO}_2\text{-Nd}_2\text{O}_3$  by melt quenching method and to study their electrical properties depending on processing temperature and composition.

## II. Experimental

The nominal compositions of the selected samples in the system  $\text{Bi}_2\text{O}_3\text{-TiO}_2\text{-SiO}_2\text{-Nd}_2\text{O}_3$ , are given in Table 1 and Fig. 1. The melting is done in alumina crucibles at the temperature between 1250 and 1500 °C for 10–15 min depending on the composition. The samples are synthesized by fast cooling to room temperature, performed by pouring of the melts between two cooper plates (with cooling rate nearly  $10^2$  °C/s). The phase formation is studied by X-ray diffraction analysis (XRD - TUR M62, Cu-K $\alpha$  radiation and Bruker D8 Advanced Diffractometer). Chemical composition is determined by energy dispersive spectroscopy (EDS, EDAX 9900). The microstructure is observed by scanning electron microscopy (SEM-525M, Philips). The electrical conductivity, capacitance and dielectric losses of the selected samples

are measured by DC resistible bridge and digital capacity meter E8-4 (1 kHz) using the two-terminal method and a suitable sample holder with graphite electrodes.

## III. Results and discussion

### 3.1 Phase formation

The obtained samples are identified as polycrystalline ceramics (Table 1, samples 1, 2, 3, 5, 6, 7, 8, 9, 10, 11, 12, 4C, 4D, 4E) or partially crystallized materials (glass-ceramics) because they have visually crystalline milk like parts and dark or transparent glass regions (Table 1, samples 4, 4A, 4B). These results are also shown in the investigated sections of the system  $\text{Bi}_2\text{O}_3\text{-TiO}_2\text{-SiO}_2\text{-Nd}_2\text{O}_3$  at 0, 5, 10 and 20 mol%  $\text{SiO}_2$ . According to the X-ray data (Fig. 2 and Table 1) several phases are identified including  $\text{Bi}_2\text{Ti}_2\text{O}_7$  (JCPDS 32-0118),  $\text{Bi}_4\text{Ti}_3\text{O}_{12}$  (JCPDS 73-2181),  $\text{Bi}_{12}\text{TiO}_{20}$  (JCPDS 78-1158) and  $\delta\text{-Bi}_2\text{O}_3$  (JCPDS 27-0052).

The increase of the  $\text{TiO}_2$  content (above 50 mol%) and the decrease of the  $\text{Bi}_2\text{O}_3$  content (below 40 mol%) leads to formation of the main phase  $\text{Bi}_4\text{Ti}_3\text{O}_{12}$ . At high  $\text{Bi}_2\text{O}_3$  content (in the range 40–60 mol%) the identified phases are  $\text{Bi}_4\text{Ti}_3\text{O}_{12}$ ,  $\text{Bi}_{12}\text{TiO}_{20}$  and  $\delta\text{-Bi}_2\text{O}_3$ . The sample 4 (Fig. 2d) is presented as an example of partially crystalline material as its X-ray diffraction pattern

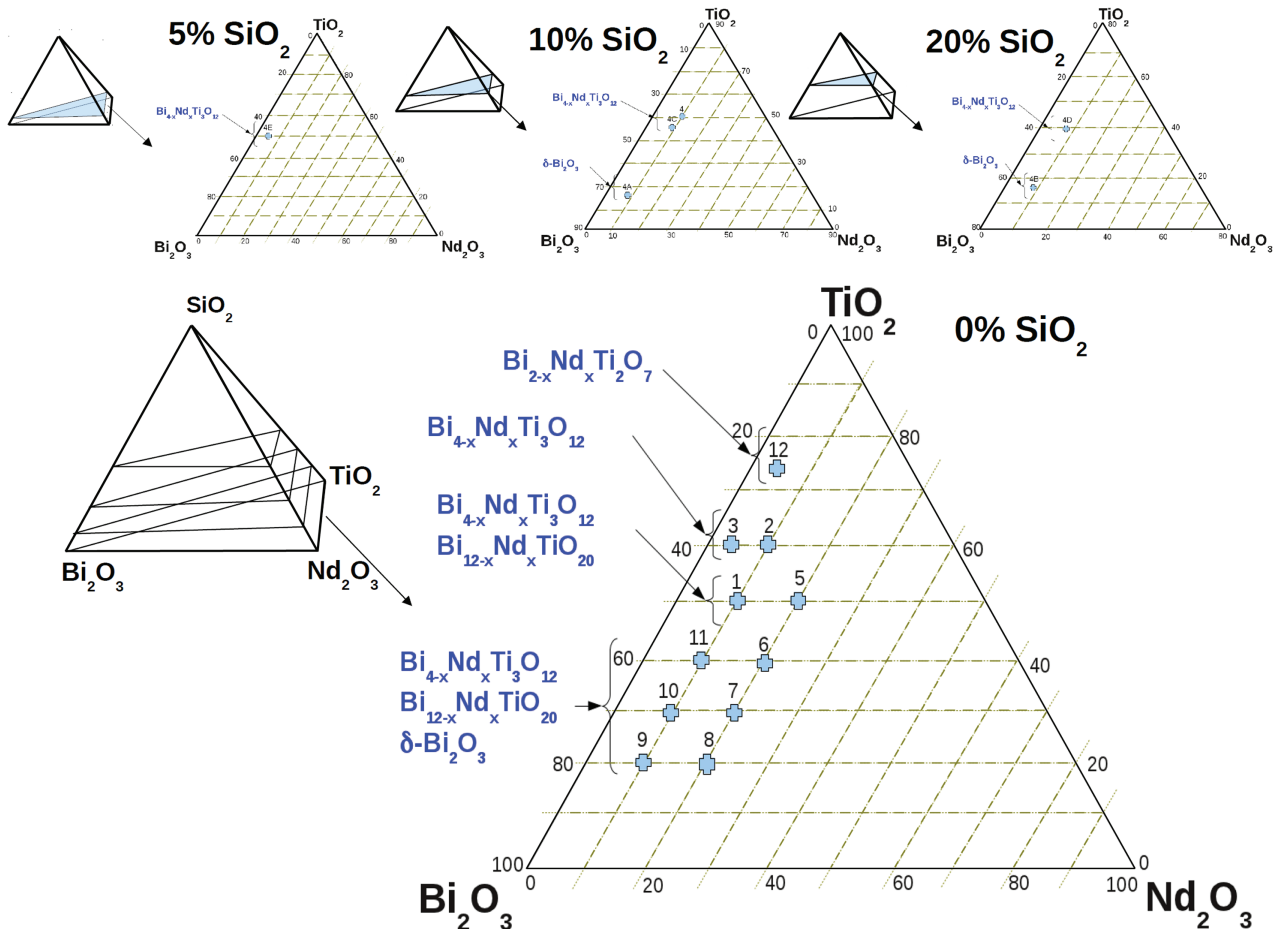


Figure 1. Investigated compositions in the system  $\text{Bi}_2\text{O}_3\text{-TiO}_2\text{-SiO}_2\text{-Nd}_2\text{O}_3$  at selected sections contains 0, 5, 10 and 20 mol%  $\text{SiO}_2$

Table 1. Starting compositions and identified phases

Sample	Starting composition [mol%]				Identified phases by XRD
	Bi <sub>2</sub> O <sub>3</sub>	TiO <sub>2</sub>	Nd <sub>2</sub> O <sub>3</sub>	SiO <sub>2</sub>	
1	40	50	10	--	Bi <sub>4</sub> , Bi <sub>12</sub>
2	25	65	10	--	Bi <sub>4</sub>
3	35	60	5	--	Bi <sub>4</sub>
4	30	50	10	10	Glass + Bi <sub>4</sub>
5	30	50	20	--	Bi <sub>4</sub> , Bi <sub>12</sub>
6	40	40	20	--	Bi <sub>4</sub> , Bi <sub>12</sub> , δ
7	50	30	20	--	Bi <sub>4</sub> , Bi <sub>12</sub> , δ
8	60	20	20	--	Bi <sub>4</sub> , Bi <sub>12</sub> , δ
9	70	20	10	--	Bi <sub>4</sub> , Bi <sub>12</sub> , δ
10	60	30	10	--	Bi <sub>4</sub> , Bi <sub>12</sub> , δ
11	50	40	10	--	Bi <sub>4</sub> , Bi <sub>12</sub> , δ
12	21	72	7	--	P
4A	63	18	10	9	Glass + δ
4B	56	16	20	8	Glass + δ
4C	36	45	10	9	Bi <sub>4</sub>
4D	32	40	20	8	Bi <sub>4</sub>
4E	40	50	5	5	Bi <sub>4</sub>

P: Bi<sub>2</sub>Ti<sub>2</sub>O<sub>7</sub>, Bi<sub>4</sub>: Bi<sub>4</sub>Ti<sub>3</sub>O<sub>12</sub>, Bi<sub>12</sub>: Bi<sub>12</sub>TiO<sub>20</sub>, δ: δ-Bi<sub>2</sub>O<sub>3</sub>

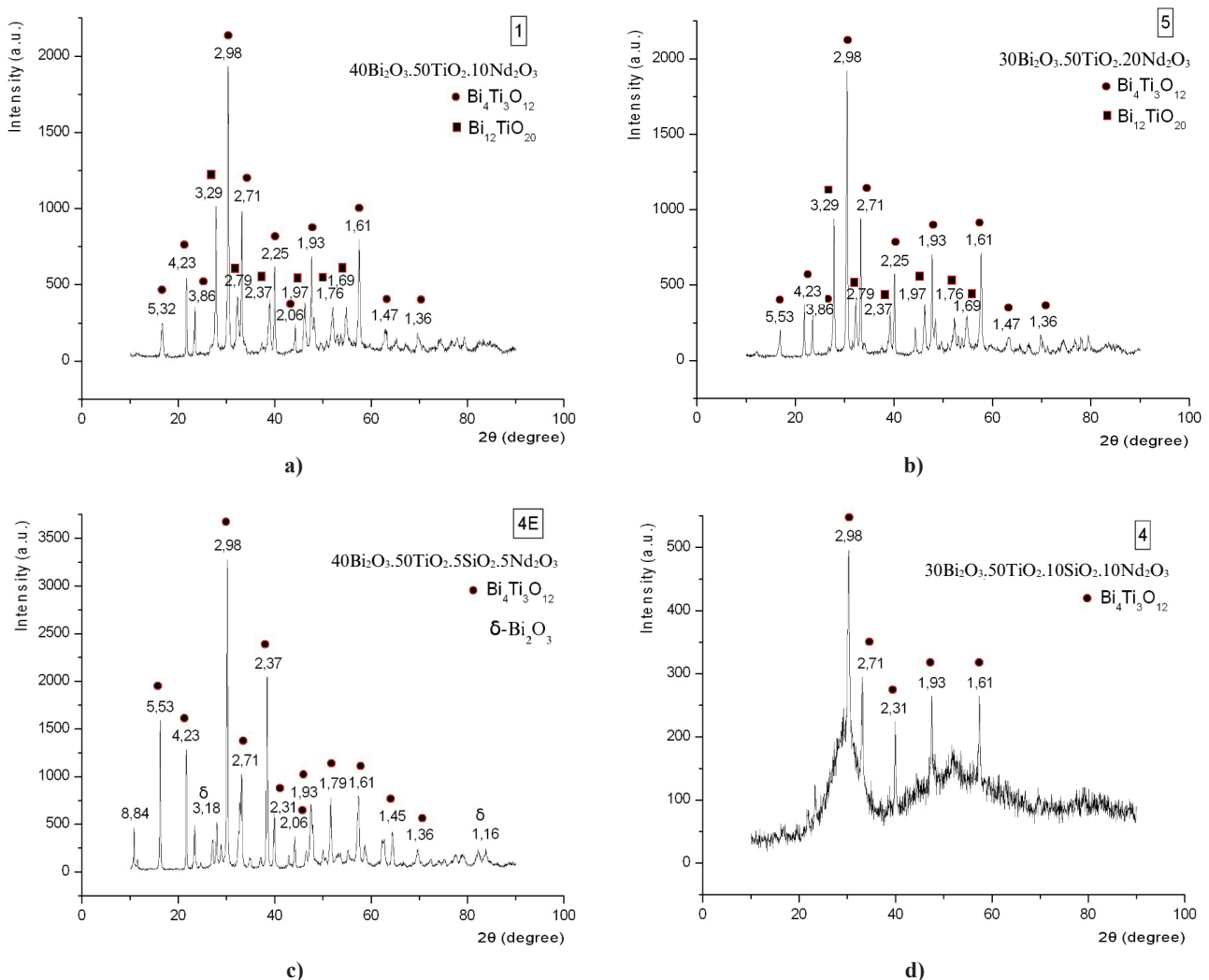


Figure 2. XRD patterns of samples with different compositions: a) 40Bi<sub>2</sub>O<sub>3</sub>·50TiO<sub>2</sub>·10Nd<sub>2</sub>O<sub>3</sub> melted at 1450 °C and fast cooled, b) 30Bi<sub>2</sub>O<sub>3</sub>·50TiO<sub>2</sub>·20Nd<sub>2</sub>O<sub>3</sub> melted at 1500 °C and fast cooled, c) 40Bi<sub>2</sub>O<sub>3</sub>·50TiO<sub>2</sub>·5SiO<sub>2</sub>·5Nd<sub>2</sub>O<sub>3</sub> melted at 1450 °C and fast cooled, and d) 30Bi<sub>2</sub>O<sub>3</sub>·50TiO<sub>2</sub>·10SiO<sub>2</sub>·10Nd<sub>2</sub>O<sub>3</sub> melted at 1450 °C and fast cooled

shows the peaks of  $\text{Bi}_4\text{Ti}_3\text{O}_{12}$  phase and an amorphous halo. Additional information about the microstructure was obtained by SEM imaging (Fig. 3). The main observed phase is a solid-solution  $\text{Bi}_{4-x}\text{Nd}_x\text{Ti}_3\text{O}_{12}$ , in which the content of  $\text{Nd}_2\text{O}_3$  varies between 9–18 mol%. These results are in agreement with the data of Kunej *et al.* [19]. They determined the upper solubility boundary to be 26 mol%  $\text{Nd}_2\text{O}_3$  instead of  $\text{Bi}_2\text{O}_3$  in the structure of  $\text{Bi}_4\text{Ti}_3\text{O}_{12}$ . In Fig. 3d it is shown that the amorphous phase contains  $\text{Bi}_2\text{O}_3$  (around 23–26 mol%),  $\text{TiO}_2$  (about 51–52 mol%),  $\text{SiO}_2$  (around 12–13 mol%) and  $\text{Nd}_2\text{O}_3$  (9–12 mol%).

### 3.2 Electrical characteristics

To compare the electrical properties, we selected four samples from the system  $\text{Bi}_2\text{O}_3$ - $\text{TiO}_2$ - $\text{SiO}_2$ - $\text{Nd}_2\text{O}_3$  with similar content of  $\text{Bi}_2\text{O}_3$  and  $\text{TiO}_2$ . The compositions of the first two of them are  $30\text{Bi}_2\text{O}_3 \cdot 50\text{TiO}_2 \cdot x\text{SiO}_2 \cdot y\text{Nd}_2\text{O}_3$ , ( $x=10, 0$ ;  $y=10, 20$ ) and the second two are formulated as:  $40\text{Bi}_2\text{O}_3 \cdot 50\text{TiO}_2 \cdot x\text{SiO}_2 \cdot y\text{Nd}_2\text{O}_3$ , ( $x=5, 0$ ;  $y=5, 10$ ). Additionally we measured the electrical properties of two samples synthesized in our previous studies:

$30\text{Bi}_2\text{O}_3 \cdot 50\text{TiO}_2 \cdot 20\text{SiO}_2$ , and  $40\text{Bi}_2\text{O}_3 \cdot 50\text{TiO}_2 \cdot 10\text{SiO}_2$  [21,22]. Arrhenius plots showing the temperature dependence of the conductivity are presented in Fig. 4. It is shown that the glass-crystalline sample containing 20 mol%  $\text{SiO}_2$  possesses the highest value of the conductivity.

The increase of the  $\text{Nd}_2\text{O}_3$  content up to 10 mol% increases the activation energy and the increase of the  $\text{SiO}_2$  content up to 10 mol% decreases the activation energy. Co-addition of  $\text{SiO}_2$  and  $\text{Nd}_2\text{O}_3$  up to 5 mol% leads to the activation energy with value close to 1 eV in the temperature range of  $1.2\text{--}2 \times 10^3 \text{ K}^{-1}$ . Further increase of the  $\text{SiO}_2$  and  $\text{Nd}_2\text{O}_3$  content to 10 mol% leads to the activation energy of 1.7 eV in temperature range  $1.2\text{--}2 \times 10^3 \text{ K}^{-1}$ .

The sample containing 20 mol%  $\text{SiO}_2$  is characterised by higher dielectric constant (Fig. 5). The decrease of the  $\text{SiO}_2$  content from 20% to 10% leads to the decrease of the dielectric constant ( $\epsilon_r$ ), but the mixed samples containing  $\text{SiO}_2$  and  $\text{Nd}_2\text{O}_3$  have higher dielectric constant at 820 °C.

More experiments need to be done in order to verify dielectric behaviour of these ceramics, which are now in course.

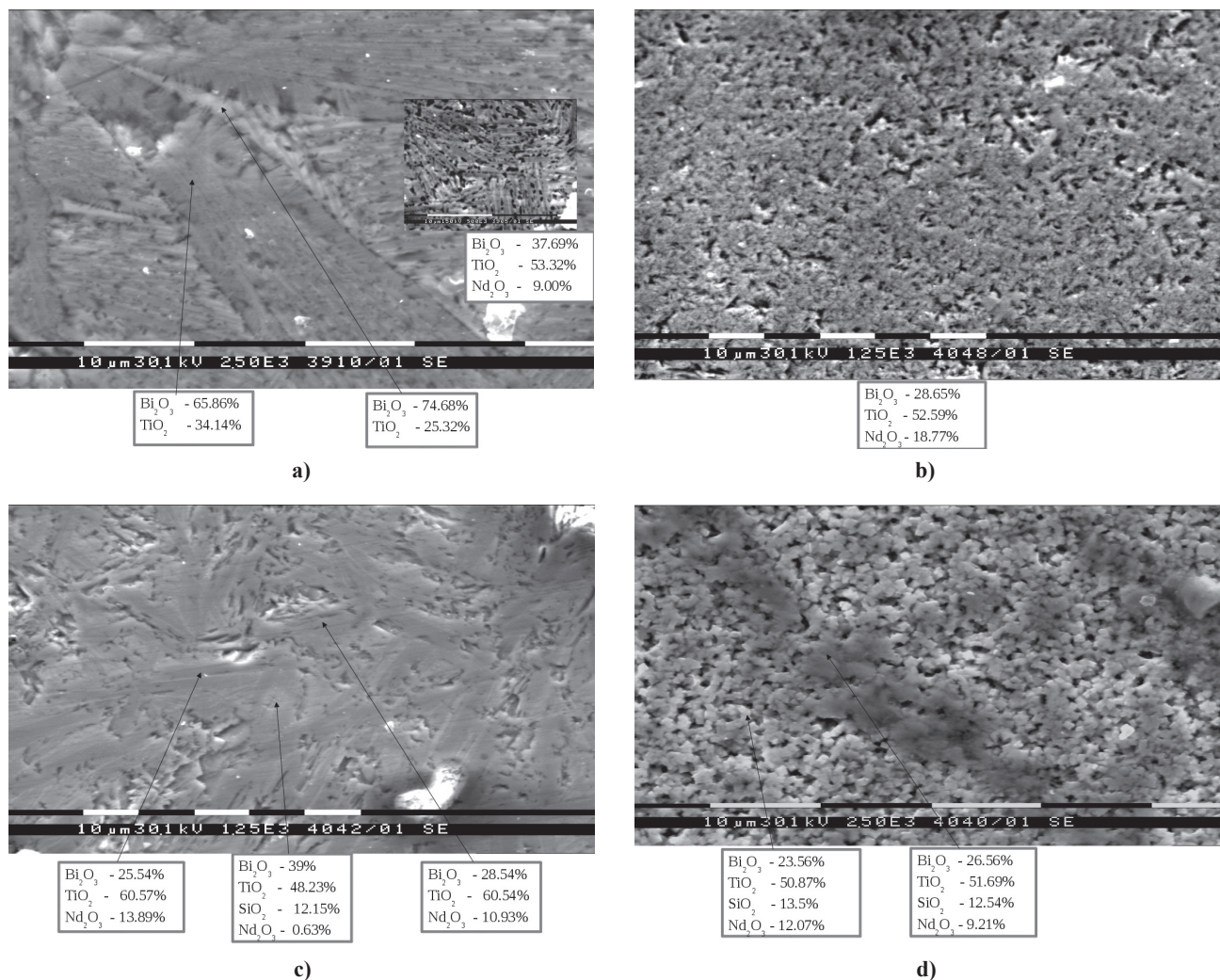


**Figure 3.** SEM micrograph and EDS data of samples with different compositions: a)  $40\text{Bi}_2\text{O}_3 \cdot 50\text{TiO}_2 \cdot 10\text{Nd}_2\text{O}_3$  melted at 1450 °C and fast cooled, b)  $30\text{Bi}_2\text{O}_3 \cdot 50\text{TiO}_2 \cdot 20\text{Nd}_2\text{O}_3$  melted at 1500 °C and fast cooled, c)  $40\text{Bi}_2\text{O}_3 \cdot 50\text{TiO}_2 \cdot 5\text{SiO}_2 \cdot 5\text{Nd}_2\text{O}_3$  melted at 1450 °C and fast cooled and d)  $30\text{Bi}_2\text{O}_3 \cdot 50\text{TiO}_2 \cdot 10\text{SiO}_2 \cdot 10\text{Nd}_2\text{O}_3$  melted at 1450 °C and fast cooling

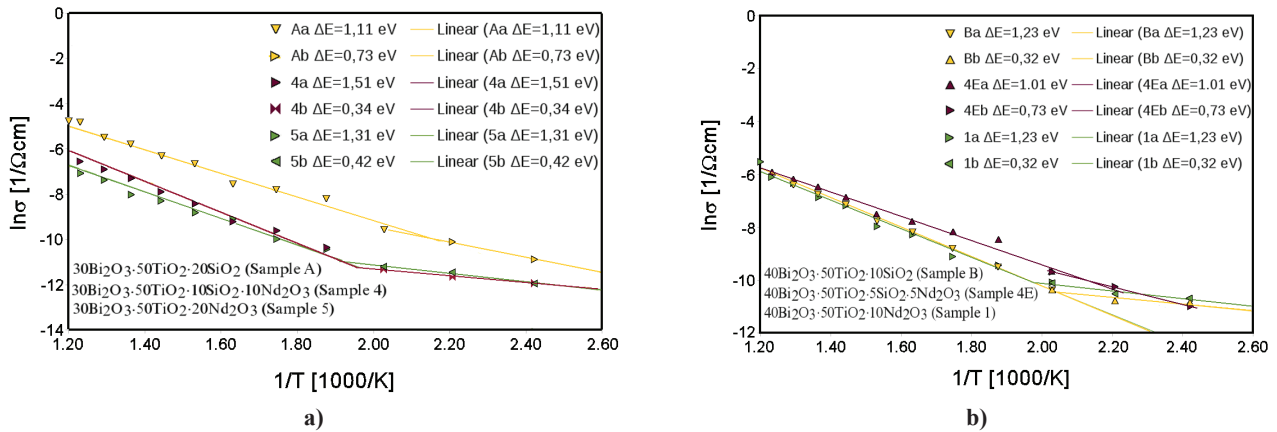


Figure 4. Arrhenius plots showing the temperature dependence of the conductivity for samples with different compositions: a)  $30\text{Bi}_2\text{O}_3 \cdot 50\text{TiO}_2 \cdot 20\text{SiO}_2$  (sample A),  $30\text{Bi}_2\text{O}_3 \cdot 50\text{TiO}_2 \cdot 10\text{SiO}_2 \cdot 10\text{Nd}_2\text{O}_3$  (sample 4) and  $30\text{Bi}_2\text{O}_3 \cdot 50\text{TiO}_2 \cdot 20\text{Nd}_2\text{O}_3$  (sample 5) and b)  $40\text{Bi}_2\text{O}_3 \cdot 50\text{TiO}_2 \cdot 10\text{SiO}_2$  (sample B),  $40\text{Bi}_2\text{O}_3 \cdot 50\text{TiO}_2 \cdot 5\text{SiO}_2 \cdot 5\text{Nd}_2\text{O}_3$  (sample 4E) and  $40\text{Bi}_2\text{O}_3 \cdot 50\text{TiO}_2 \cdot 10\text{Nd}_2\text{O}_3$  (sample 1)

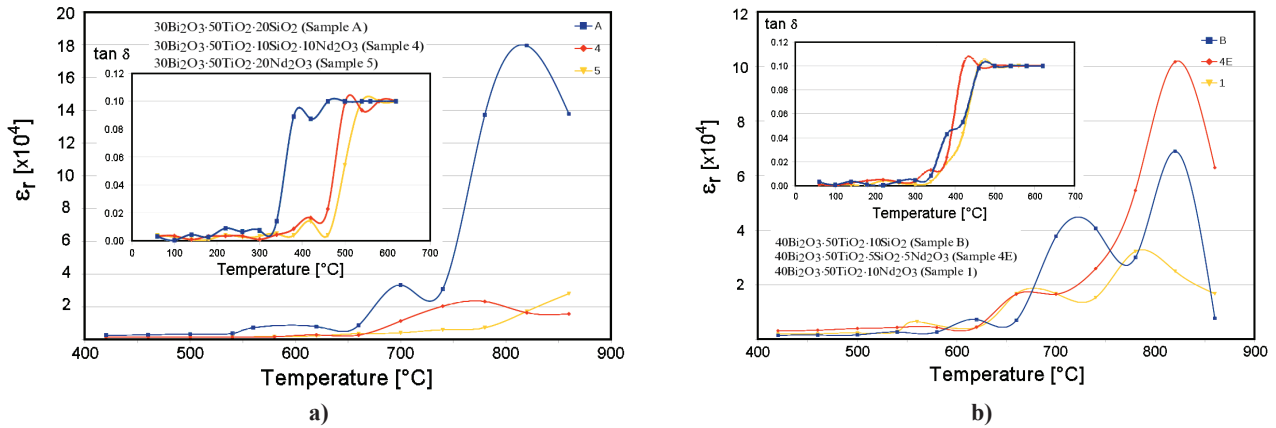


Figure 5. Plot of the relative permittivity and dielectric losses in dependence on the temperature for samples with different compositions: a)  $30\text{Bi}_2\text{O}_3 \cdot 50\text{TiO}_2 \cdot 20\text{SiO}_2$  (sample A),  $30\text{Bi}_2\text{O}_3 \cdot 50\text{TiO}_2 \cdot 10\text{SiO}_2 \cdot 10\text{Nd}_2\text{O}_3$  (sample 4) and  $30\text{Bi}_2\text{O}_3 \cdot 50\text{TiO}_2 \cdot 20\text{Nd}_2\text{O}_3$  (sample 5) and b)  $40\text{Bi}_2\text{O}_3 \cdot 50\text{TiO}_2 \cdot 10\text{SiO}_2$  (sample B),  $40\text{Bi}_2\text{O}_3 \cdot 50\text{TiO}_2 \cdot 5\text{SiO}_2 \cdot 5\text{Nd}_2\text{O}_3$  (sample 4E) and  $40\text{Bi}_2\text{O}_3 \cdot 50\text{TiO}_2 \cdot 10\text{Nd}_2\text{O}_3$  (sample 1)

#### IV. Conclusions

The investigation carried out confirms that depending on the melting conditions of the super-cooled melt different poly-phase glass-ceramic materials with various microstructures could be obtained containing mainly the bismuth titanate phases in the system  $\text{Bi}_2\text{O}_3$ - $\text{TiO}_2$ - $\text{Nd}_2\text{O}_3$ - $\text{SiO}_2$ . The addition of  $\text{Nd}_2\text{O}_3$  in the samples leads to the increase of the melting temperature and decreases the tendency to form glassy structure. It is established that all investigated samples are dielectric materials with conductivity between  $10^{-9}$  and  $10^{-13}$  ( $\Omega \cdot \text{cm}$ ) $^{-1}$  at room temperature, dielectric permittivity in the range of 1000 to 3000 and dielectric losses  $\text{tg} \delta$  between 0.0002 and 0.1. Addition of  $\text{SiO}_2$  and  $\text{Nd}_2\text{O}_3$  in the samples leads to essential changes of dielectric losses and conductivity.

**Acknowledgements:** The study was performed with financial support of UCTM, Sofia under Grant № 10979/2012.

#### References

1. C. Araujo, J. Cuchiaro, L. Mc Milan, M. Scott, J. Scott, "Fatigue free-ferroelectric capacitors with platinum electrodes", *Lett. Nature*, **374** (1995) 627–629.
2. B.H. Park, B.S. Kang, S.D. Bu, T.W. Noh, J. Lee, W. Jo, "Lanthanum-substituted bismuth titanate for use in non-volatile memories", *Lett. Nature*, **401** (1999) 682–684.
3. S. Kojima, A. Hushur, F. Jiang, S. Hamazaki, M. Takashige, M. Jang, S. Shimada, "Crystallization of amorphous bismuth titanate", *J. Non-Cryst. Solids*, **293-295** (2001) 250–254.
4. K. Sunahara, J. Yano, K. Kakegawa, "Preparation of  $\text{Bi}_4\text{Ti}_3\text{O}_{12}$  particles by crystallization from glass", *J. Eur. Ceram. Soc.*, **26** (2006) 623–626.
5. K. Gerth, Ch. Russel, "Crystallization of  $\text{Bi}_4\text{Ti}_3\text{O}_{12}$  from glasses in the system  $\text{Bi}_2\text{O}_3/\text{TiO}_2/\text{B}_2\text{O}_3$ ", *J. Non-Cryst. Solids*, **221** (1997) 10–17.
6. K. Gerth, Ch. Russel, "Crystallization of  $\text{Bi}_3\text{TiNbO}_9$  from glasses in the system  $\text{Bi}_2\text{O}_3/\text{TiO}_2/\text{Nb}_2\text{O}_5/\text{B}_2\text{O}_3/\text{SiO}_2$ ", *J. Non-Cryst. Solids*, **243** (1999) 52–60.

7. H. Maiwa, N. Lizawa, D. Togawa, W. Sakamoto, M. Yamada, S-I. Hirano, T. Hayashi, "Electromechanical properties of Nd-doped  $\text{Bi}_4\text{Ti}_3\text{O}_{12}$  films: A candidate for lead-free thin film piezoelectric", *J. Appl. Phys.*, **A 82** [11] (2003) 1760–1762.
8. G. Suyal, S.S.N. Bharadwaja, M. Cantoni, D. Damjanovic, N. Setter, "Properties of chemical solution deposited polycrystalline neodymium-modified  $\text{Bi}_4\text{Ti}_3\text{O}_{12}$ ", *J. Electroceram.*, **9** (2002) 187–192.
9. Q-Y. Tang, Y-M. Kan, P-L. Wang, Y-G. Li, G-J. Zhang, "Nd/V Co-doped  $\text{Bi}_4\text{Ti}_3\text{O}_{12}$  power prepared by molten salt synthesis", *J. Am. Ceram. Soc.*, **90** [10] (2007) 3353–3356
10. T. Kojima, T. Sakai, T. Watanabe, H. Funakudo, "Large remanent polarization of  $(\text{Bi},\text{Nd})_4\text{Ti}_3\text{O}_{12}$  epitaxial thin films grown by metalorganic chemical vapor deposition", *Appl. Phys. Lett.*, **80** [15] (2002) 2746–2748.
11. J.K. Kim, S.S. Kim, W.J. Kim, "Effects of annealing conditions on the electrical properties of  $\text{Bi}_{4-x}\text{Nd}_x\text{Ti}_3\text{O}_{12}$  ( $x=0.46$ ) thin films processed at low temperature", *J. Appl. Phys.*, **A 82** (2006) 737–740.
12. W. Sakamoto, M. Yamada, N. Iizawa, Y-K. Muzutani, D. Togaza, K. Kikuta, T. Yogo, T. Hayashi, S-I. Hirano, "Preparation and properties of  $\text{Bi}_{4-x}\text{Nd}_x\text{Ti}_3\text{O}_{12}$  thin films by chemical solution deposition", *J. Electroceram.*, **13** (2004) 339–343.
13. D. Wu, A. Li, N. Ming, "Structure and electrical properties of  $\text{Bi}_{3.15}\text{Nd}_{0.85}\text{Ti}_3\text{O}_{12}$  ferroelectric thin films", *J. Appl. Phys.*, **A 95** [8] (2004) 4275–4281.
14. M. Chen, Z.L. Liu, Y. Wang, C.C. Wang, X.S. Yang, K.L. Yao: "Ferroelectric properties and microstructures of  $\text{Nd}_2\text{O}_3$ -doped  $\text{Bi}_4\text{Ti}_3\text{O}_{12}$  ceramics", *Phys. Stat. Sol. A - Appl. Res.*, **200** (2003) 446–450.
15. J.L. Pinede-Flores, E. Chavira, J. Reyes-Gasga, A.M. Gonzalez, A. Huanosta-Tera, "Synthesis and dielectric characteristics of the layered structure  $\text{Bi}_{4-x}\text{R}_x\text{Ti}_3\text{O}_{12}$  ( $\text{R}_x = \text{Pr, Nd, Gd, Dy}$ )", *J. Eur. Ceram. Soc.*, **23** (2003) 839–850.
16. N.V. Giridharan, M. Subramanian, R. Jayavel, "Enhancement of polarization in bismuth titanate thin films co-modified by La and Nd for non-volatile memory application", *J. Appl. Phys.*, **A 83** (2006) 123–126.
17. J. Li, J. Yu, G. Peng Y. Wang, W. Zhou, "Effect of  $\text{TiO}_2$  seeding layer on crystalline orientation and ferroelectric properties of  $\text{Bi}_{3.15}\text{Nd}_{0.85}\text{Ti}_3\text{O}_{12}$  thin films fabricated by a sol-gel method", *J. Am. Ceram. Soc.*, **90** [10] (2007) 3220–3223.
18. L. Jiao, Z. Liu, G. Hu, S. Cui, S. Jin, Q. Wang, W. Wu, C. Yang, "Low-temperature fabrication and enhanced ferro- and piezoelectric properties of  $\text{Bi}_{3.7}\text{Nd}_{0.3}\text{Ti}_3\text{O}_{12}$  films on indium tin oxide/glass substrates", *J. Am. Ceram. Soc.*, **92** [7] (2009) 1556–1559.
19. S. Kunej, S. Skapin, D. Suvorov, "Phase relations in the pyrochlore-rich part of the  $\text{Bi}_2\text{O}_3$ - $\text{TiO}_2$ - $\text{Nd}_2\text{O}_3$  system", *J. Am. Ceram. Soc.*, **92** [10] (2009) 2373–2377.
20. M. Krapchanska, Y. Dimitriev, R. Iordanova, "Phase formation in the system  $\text{Bi}_2\text{O}_3$ - $\text{TiO}_2$ - $\text{SiO}_2$ ", *J. Univ. Chem. Technol. Metal.*, **43** (2006) 307–310.
21. E. Kashchieva, M. Krapchanska, S. Slavov, Y. Dimitriev, "Effect of synthesis route on the microstructure of  $\text{SiO}_2$  doped bismuth titanate ceramics", *Process. Applic. Ceram.*, **3** [4] (2009) 171–175.
22. S. Slavov, M. Krapchanska, E. Kashchieva, Y. Dimitriev, "Electrical characteristics of bismuth titanate ceramics containing  $\text{SiO}_2$  and  $\text{Nd}_2\text{O}_3$ ", *Process. Applic. Ceram.*, **4** [1] (2010) 39–43.